Continuous Comagnetometry using Transversely Polarized Xe Isotopes

D. Thrasher,[1] S. Sorensen,[1] J. Weber,[2] M. Bulatowicz,[1] A. Korver,[1] M. Larsen,[3] and T. G. Walker[1]

[1]*Department of Physics, University of Wisconsin-Madison, Madison, Wisconsin 53706, USA*
[2]*Natural Sciences Department, Parkland College, Champaign, IL 61821, USA*
[3]*Northrop Grumman, Advanced Position, Navigation and Timing Systems, Woodland Hills, CA 91367, USA*
(Dated: October 8, 2019)

We demonstrate a transversely polarized spin-exchange pumped noble gas comagnetometer which suppresses systematic errors from longitudinal polarization. Rb atoms as well as ^{131}Xe and ^{129}Xe nuclei are simultaneously polarized perpendicular to a pulsed bias field. Both Xe isotopes' nuclear magnetic resonance conditions are simultaneously satisfied by frequency modulation of the pulse repetition rate. The Rb atoms detect the Xe precession. We highlight the importance of magnetometer phase shifts when performing comagnetometry. For detection of non-magnetic spin-dependent interactions the sensing bandwidth is 1 Hz, the white-noise level is 7 μHz $/\sqrt{\text{Hz}}$, and the bias stability is ≈ 1 μHz.

Spin-exchange (SE) pumped comagnetometers [1, 2] utilize co-located ensembles of spin-polarized alkali-metal atoms and noble gas nuclei [3] to suppress magnetic field noise. Such devices have been used to place upper bounds on spin-mass couplings [4, 5], Lorentz violations [6–10], and nuclear electric dipole moments [11–13], and for the measurement of inertial rotation [2, 14–16]. The fundamental uncertainty of a SE pumped comagnetometer's measure of inertial rotation scales favorably with sensor size compared to alternative technologies [17].

Longitudinal SE fields are important sources of systematic uncertainty in devices which utilize the embedded alkali-metal atoms for high SNR detection. Consider an ensemble of two noble gas species (a and b) which are spin-exchange optically pumped (SEOP) in a common magnetic field B_z and are each subject to some spin-dependent interaction X. The Larmor resonance frequency of isotope a can be written as [2, 18–20]

$$\Omega^a = \gamma^a \left(B_z + b_S^a S_z + b_b^a K_z^b \right) + X_z^a, \qquad (1)$$

where γ is the gyromagnetic ratio, S and K are the respective alkali-metal and noble gas polarizations, z subscripts refer to the longitudinal components (*i.e.*, parallel to the bias field direction), and b_j^i is the SE coefficient characterizing the influence of j's polarization on i. With knowledge of $\rho = \gamma^a/\gamma^b$, simultaneous measurement of Ω^a and Ω^b allows B_z to be suppressed while sensitivity to X_z^a and X_z^b is retained [21].

In this paper we demonstrate a SE pumped ^{131}Xe-^{129}Xe comagnetometer which suppresses time-averaged S_z and K_z such that

$$\xi \equiv \frac{\rho\Omega^b - \Omega^a}{1 + \rho} \approx \frac{\rho X_z^b - X_z^a}{1 + \rho}, \qquad (2)$$

where the superscripts a and b refer to ^{129}Xe and ^{131}Xe, respectively, and $\rho = 3.3734$ [22]. The comagnetometer relies on a dual-species version of synchronous SEOP [23], wherein noble gas nuclei are continuously polarized transverse to a frequency modulated pulsed bias field. We demonstrate that the correlation between the frequency of precession of ^{131}Xe and ^{129}Xe is sufficient to resolve 7
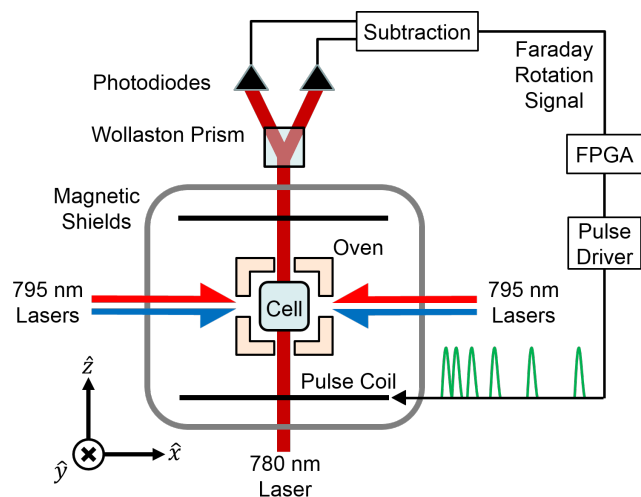

FIG. 1: Schematic of apparatus. Field shim coils are not shown. The green trace depicts the frequency modulated bias field pulses.

μHz $/\sqrt{\text{Hz}}$ of white frequency noise with a low frequency field noise suppression of $> 10^3$. We also demonstrate the influence of alkali-metal magnetometer phase shifts on the field noise suppression of the comagnetometer.

A schematic of the experimental setup is shown in Fig. 1. ^{85}Rb atoms are optically pumped along $\hat{x}$, transverse to a pulsed bias field oriented along $\hat{z}$. The noble gas nuclei are polarized via SE collisions with the Rb atoms. The bias field is applied as a series of low duty cycle pulses (depicted in green), where each pulse produces a 2π Larmor rotation of the Rb spins. Due to the $\sim 10^3$-fold smaller magnetic moments of the Xe isotopes, they experience an effective bias field of $B_p(t) = \omega_p(t)/\gamma^S$, where $\omega_p(t)$ is the repetition rate of the 2π pulses and $\hbar\gamma^S = 2\mu_B/(2I + 1)$, where $I = 5/2$ is the ^{85}Rb nuclear spin and μ_B is the Bohr magneton. The magnetic resonance of each noble gas species is simultaneously excited by modulating ω_p at linear combinations of Ω^a and Ω^b.
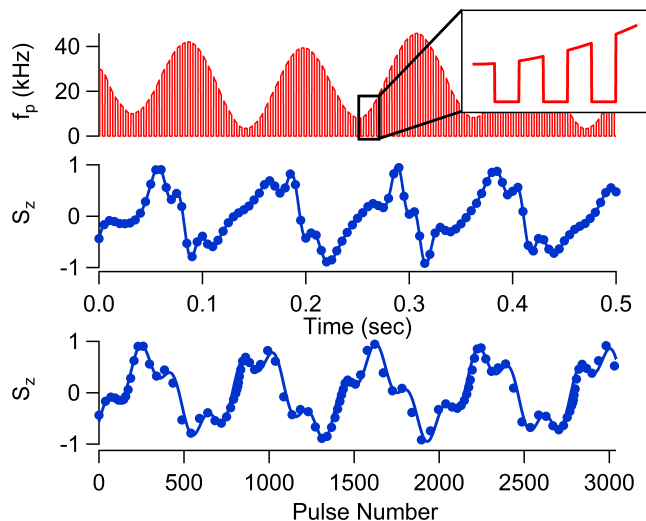
The experimental apparatus is similar to Ref. [23]. Up-

FIG. 2: Time dependence of bias pulse repetition rate f_p (top) and normalized S_z (middle) for $\Delta^a = \Delta^b \approx 0$. Corresponding pulse number dependence of normalized S_z (bottom). Filled circles are measured data. Lines are theory fits to the data. Inset depicts greater time detail of the bias pulse gating.

dates include an 8 mm cubic Pyrex cell filled with 40 Torr enriched Xe and 50 Torr N_2 with a hydride coating [24], and a custom-made pulse driver designed so that the voltage required to produce 2π pulses is largely independent of pulse repetition rate.

The embedded Rb magnetometer, which is effectively at zero-field due to the low duty cycle nature of the bias field pulses [25], continuously detects the noble gas SE field $b_K^S K_y$. The Faraday rotation of a linearly polarized probe laser propagating parallel to the bias field serves as a monitor of $S_z \propto K_y$. The S_z signal is digitally demodulated, and the pulse modulation frequencies are adjusted to maintain resonance for both Xe species. The Xe resonance frequencies determined by the feedback are recorded and used to compute ξ.

We optically pump the Rb atoms with circularly polarized light propagating along $\pm\hat{x}$. We take care to null transverse fields experienced by the Xe, including the SE field $b_S^K S_x$, such that the longitudinal components of the Xe polarizations are negligible [23]. Under these conditions, the transverse components $K_+ = K_x + iK_y$ of the nuclear spin polarization for each noble gas species obey

$$\frac{dK_+}{dt} = -(\mp i\Omega + \Gamma_2)K_+ + \Gamma_S^K S_+ \qquad (3)$$

where $\Omega = \gamma B_z + X_z$ is the Larmor resonance frequency, arising from both magnetic field B_z and spin-dependent phenomena X_z. The SE rate constant is Γ_S^K, and the transverse relaxation rate is Γ_2. The sign in front of Ω encodes the direction of precession (top is ^{129}Xe, bottom is ^{131}Xe). We assume that ^{131}Xe frequency shifts due to quadrupole interactions are independent of B_z and are included in X_z^b.

Multiple noble gas species can be simultaneously excited via SE collisions with the Rb by modulating either S_+ [23] or B_z. Here we choose to modulate B_z by modulating ω_p. The Rb magnetometer is far less sensitive to changes in ω_p than to changes in DC fields.

The magnetic field component along $\hat{z}$ is $B_z = B_{z0} + B_p(t)$, which consists of the stray field B_{z0} and the field from the 2π pulses $B_p(t) = B_{p0} + B_m(t)$, where B_{p0} is the DC component and B_m is the AC component of the pulsed field. Since each pulse produces 2π precession of the Rb atoms, the Rb atoms primarily experience B_{z0}, while the Xe nuclei experience both B_{z0} and B_p. In practice, we find that the magnetometer gain varies up to a factor of two as the pulse repetition rate is modulated (the magnetometer would not function if B_{z0} were modulated instead). We avoid such gain modulation by gating the 2π pulses and only recording the Faraday signal when the pulses are off and the magnetometer gain has stabilized. The 2π pulse repetition rate (depicted in Fig. 2) is modulated as

$$\omega_p(t) = \omega_{p0}g(t)(1 + b_1\cos(\omega_1 t) + b_2\cos(\omega_2 t)), \quad (4)$$

where $g(t) = (\mathrm{sign}(\cos(\omega_3 t)) + 1)$ is the time dependence of the gating, $\omega_1 = \omega_d^b$ and $\omega_2 = \omega_d^a - 3\omega_d^b$ determine the Xe drive frequencies, and b_1 and b_2 set the depth of modulation.

Though the Rb atoms are optically pumped along $\hat{x}$, the field B_{z0} causes their polarization to rotate slightly into $\hat{y}$. This tip causes a phase shift in the drive of each isotope as well the detection of their precession. The transverse spin is then $S_+ = S_\perp e^{i\epsilon_z}$, where $\epsilon_z = \tan^{-1}(\frac{S_y}{S_x}) \approx \tan^{-1}(\frac{B_{z0}}{B_w})$ is the magnetometer phase shift due to B_{z0} and B_w is the magnetic width of the magnetometer.

We use a phasor representation $K_+ = K_\perp e^{\pm i\phi}$ for the nuclear spin polarization. In the experiment we measure the difference $\delta = \phi - \alpha$ between the instantaneous Xe phase ϕ and a reference phase $\alpha = \int(\omega_d + \gamma B_m)dt$ which is the phase the Xe would have if the only fields present were the pulsing fields and if $\Delta \equiv \omega_d - \Omega_0 = 0$ with $\Omega_0 = \gamma(B_{z0} + B_{p0}) + X_z$. To first order in δ and ϵ_z, the imaginary part of Eq. 3 is

$$\frac{d\delta}{dt} = -\Delta - \Gamma_2(\delta \mp \epsilon_z), \qquad (5)$$

and the time average of the real part is $K_\perp = \Gamma_S^K S_\perp C / \Gamma_2$, where C is the time average of $\cos(\alpha)$. Note that the precession direction makes the sign in front of ϵ_z isotope dependent.

We detect the z-component of the Rb spin,

$$S_z = \frac{1}{B_w}(b_a^S \mathbf{K^a} \times \mathbf{S} + b_b^S \mathbf{K^b} \times \mathbf{S})_z$$
$$= A_\perp^a \sin(\phi^a - \epsilon_z) + A_\perp^b \sin(\phi^b + \epsilon_z). \qquad (6)$$

This assumes that $\mathbf{K}$ precesses slowly enough that S_z adiabatically responds. It also assumes negligible back polarization from the Xe to the Rb [1, 26]. We see that
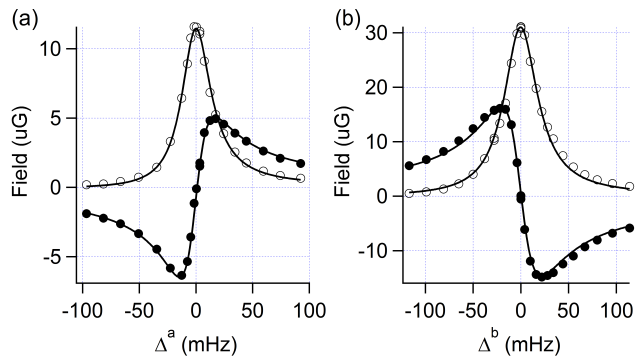
FIG. 3: Xe NMR Lineshapes. (a) $b_a^S K_\perp^a$ vs Δ^a. (b) $b_b^S K_\perp^b$ vs Δ^b. Filled circles are K_x and open circles are K_y. Lines are Lorentzian fits to the data.

the detected phase of S_z depends on the Xe phases as well as the magnetometer phase.

Figure 2 shows S_z for $\Delta^a = \Delta^b \approx 0$ as a function of both time and pulse number. Although the signal exhibits a complicated time dependence, its dependence on pulse number (which is equivalent to its dependence on α if $\Delta = 0$) is a simple superposition of sine waves. We extracted the precession phase of each isotope as measured by the Rb by demodulating S_z with $\cos(\alpha)$. Since S_z was sampled at ω_3, we applied an anti-aliasing filter before approximating the time average by a moving average over N data points, where N was chosen to remove the high frequency residuals of the demodulation.

Figure 3 shows the demodulated S_z for each isotope as ω_d is scanned, giving a familiar NMR resonance shape. The data were acquired with one isotope driven on resonance while the other isotope's detuning was varied. For the field modulation, we set $\omega_3 = 2\pi \times 200$ Hz, $b_1 = 0.73$ and $b_2 = 0.15$, and $\omega_{p0} \approx 2\pi \times 13.2$ kHz, resulting in average precession frequencies of ≈ 33.3 Hz and ≈ 9.9 Hz for ^{129}Xe and ^{131}Xe, respectively. The moving average filter was N=162. With these settings, the amplitude of B_m was about $10B_w$ and the detection bandwidth was 1 Hz.

For ^{131}Xe we realize $b_b^S K_\perp^b \approx 30$ μG (corresponding to 0.1% polarization) and a linewidth of 21.2(3) mHz. For ^{129}Xe we realize $b_a^S K_\perp^a \approx 10$ μG (0.3% polarization) and a linewidth of 15.6(3) mHz. Such low ^{129}Xe polarization relative to the Rb polarization at our Rb density ($n_S \approx 10^{13}$cm^{-3}) could be due to a temperature-dependent wall relaxation mechanism similar to what has been reported in Rb-^{3}He cells [27]. We see no signs of quadrupole beating in the ^{131}Xe signal and believe the absence of first order quadrupole beating is generic to transverse polarization. From free induction decay studies we estimate residual quadrupole effects to be 2 mHz [28].

For small fluctuations (or rotations) about the bias magnetic field, the phase δ of the Xe transverse polarization relative to Rb transverse polarization is much more strongly affected than its magnitude, and obeys Eq. 5.

Performing a Fourier transform gives

$$\tilde{\delta} = -\frac{\tilde{\Delta} \mp \Gamma_2 \tilde{\epsilon}_z}{i\omega + \Gamma_2}. \tag{7}$$

We adjust the drive frequency of each isotope to hold its measured phase to zero [29]. Doing so reduces uncertainty in the transformation from phase to frequency for each isotope. The feedback can be written

$$\tilde{\omega_d} = \tilde{G}(\tilde{\delta} \mp \tilde{\epsilon}_z) \tag{8}$$

where $\tilde{G}$ is frequency-dependent gain (units of 2π Hz/rad). The finite gain corrected drive frequency is then

$$\tilde{\omega}_d \equiv \tilde{\omega}_d \tilde{G}^{-1}(i\omega + \Gamma_2 + \tilde{G}) = \tilde{\Omega}_0 \mp i\omega\tilde{\epsilon}_z. \tag{9}$$

The comagnetometer signal ξ' is computed in post processing using the ω_d's such that $\tilde{\xi}' = \tilde{\xi} + i\omega\tilde{\epsilon}_z$, where $\omega_d^a, \omega_d^b > 0$.

To extract ξ from ξ', we assume

$$\tilde{\epsilon}_z = \tan^{-1}\left(\frac{1}{B_w} \frac{\tilde{\omega}_d^a + \tilde{\omega}_d^b}{\gamma^a + \gamma^b} \right), \tag{10}$$

which follows if $\tilde{B}_{z0}$ is the dominant contribution to both $\tilde{\epsilon}_z$ and the sum of the finite gain corrected drive frequencies. We will show that this assumption dramatically improves the comagnetometer's suppression of magnetic field noise.

We stabilize the two drive frequencies to line center with an accuracy of ±0.3 mHz and record the drive frequencies as a function of time. Once acquired, the individual drive frequencies are corrected for finite gain and used to compute ϵ_z and ξ. Figure 4 (a) shows the amplitude spectral densities of ω_d^a, ω_d^b, and ξ. The spectrum of ω_d^a is approximately ρ larger than that of ω_d^b from DC to 0.1 Hz, suggesting that $\hat{z}$ magnetic field noise dominates over this frequency band.

In separate experiments, we record the drive frequencies with an ancillary B_z applied. This 5 mHz 4.3 μG field is used to measure the field suppression factor (FSF), which we define to be $\tilde{\omega}_d^{131}/\tilde{\xi}$ at the frequency of the ancillary B_z. We find that the FSF depends critically on the assumed value of B_w (see Fig. 4 (b)), which scales ϵ_z. We measure B_w independently using two methods; from the open loop response of the Xe (see Eq. 7) we infer $B_w = 3.5(3)$ mG, and from the magnetometer's response to B_y we find $B_w = 3.1(1)$ mG. Analyzing the precession data assuming the weighted mean $B_w = 3.14$ mG we find an FSF of 470. However, choosing $B_w = 2.0$ mG produces an FSF of 2300. Alternatively, if we ignore the influence of ϵ_z completely and calculate $\tilde{\omega}_d^{131}/\tilde{\xi}'$, we find an FSF of 75. Clearly, ϵ_z introduces substantial phase shifts in the comagnetometer signal, significantly limiting the FSF if left unaccounted for.

In order to suppress uncertainty in the FSF due to B_w, we built an additional feedback loop which corrected B_{z0} such that the sum $\omega_d^a + \omega_d^b$ was kept fixed in real time. The gain of this feedback loop was sufficient to
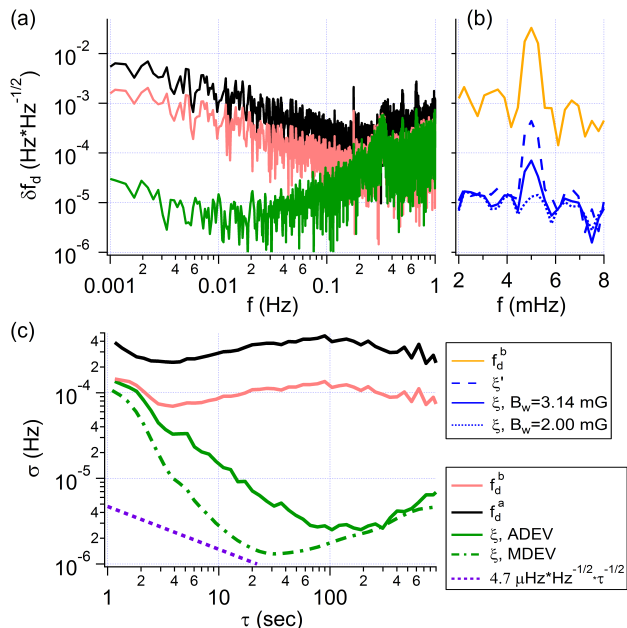
FIG. 4: (a) Amplitude spectral densities of f_d^b, f_d^a, ξ. (b) Spectra with ancillary AC B_z applied showing the field suppression factor for various comagnetometer signal computations. (c) Allan Deviations of f_d^b, f_d^a, ξ, where ξ was analyzed with both standard and modified Allan deviations. All data shown have been corrected for finite gain. A Hanning window is applied to each spectrum.

suppress $\tilde{\omega}_d^b$ by a factor of 15 at 5 mHz compared to when B_{z0} was not stabilized. The FSF was 1800 with this additional feedback loop (taking into acount the factor of 15 suppression of $\tilde{\omega}_d^b$).

Figure 4(a) shows ξ's spectrum without an ancillary B_z and without B_{z0} feedback. $\tilde{\xi}$ reaches a white noise level of $< 10\ \mu$Hz $/\sqrt{\text{Hz}}$ regardless of the B_w used in computation, suggesting that ξ's noise is not limited by the FSF ($B_w = 3.14$ mG for the data shown).

Figure 4 (c) shows the standard Allan deviation (ADEV) of ω_d^b, ω_d^a, and ξ as well as the modified Allan deviation (MDEV) [30] of ξ, each with a 1 Hz step low pass filter applied. The MDEV averages f frequency noise faster and is therefore able to resolve a lower bias

stability of roughly 1 μHz after 30 seconds of integration. Both the ADEV and MDEV eventually exhibit $\tau^{1/2}$ trends. The source of this $1/f$ frequency drift is uncertain. Possible sources of drift include contributions to ϵ_z besides B_z (which are not accounted for in our current computation of ϵ_z) and fluctuations in Γ_2 (which likely stem from Rb density fluctuations and manifest as noise if $\Delta \neq 0$ [2]).

Fitting the MDEV results [31] in an angle-random walk (ARW) of $\sqrt{2} \times 4.7(4) = 6.6(6)\ \mu$Hz$/\sqrt{\text{Hz}}$. The measured SNRs (5300 and 3200 $\sqrt{\text{Hz}}$ for ^{131}Xe and ^{129}Xe, respectively) suggest an ARW limit of 4 μHz$/\sqrt{\text{Hz}}$, very similar to that found by fitting the MDEV. The photon shot noise limited ARW is roughly a factor of 10^3 smaller. It is unclear what is currently limiting the detection noise.

This is the first demonstration of a continuously SE pumped comagnetometer which avoids time-averaged longitudinal alkali-metal and noble gas polarization. The demonstrated field suppression and white frequency noise would be sufficient to realize a bias stability of 200 nHz if stray $1/f$ magnetic noise were the dominant noise contribution. Despite 30× smaller $b_K^S K_\perp$, the ARW is only 6× that of Ref. [1] at 230× the bandwidth.

We have shown that the phase of the embedded alkali-metal magnetometer ϵ_z plays an important role in understanding the comagnetometer. Indeed, the field suppression factor improves dramatically when correcting B_{z0} to keep $\omega_d^a + \omega_d^b = const$. We note that, in addition to B_z, ϵ_z could also depend on pump pointing, K_z, and back polarization (K_y producing S_y). By measuring the response of the magnetometer to an ancillary rotating $B_\perp$, ϵ_z could be monitored directly and in real time for greater precision.

The stability demonstrated should be sufficient to make the first measurement of b_a^b [18, 32]. Additionally, with a 2 mm cell [4], we anticipate being able to improve the present upper bound for spin-mass couplings in the sub-mm wavelength range by an order of magnitude after merely 100 seconds of measurement.

ACKNOWLEDGMENTS

[1] M. E. Limes, D. Sheng, and M. V. Romalis, "^{3}He–^{129}Xe comagnetometery using ^{87}Rb detection and decoupling," Phys. Rev. Lett. **120**, 033401 (2018).

[2] T.G. Walker and M.S. Larsen, "Spin-exchange-pumped nmr gyros," Advances In Atomic, Molecular, and Optical Physics, **65**, 373 – 401 (2016).

[3] T.G. Walker and W. Happer, "Spin-exchange optical pumping of noble-gas nuclei," Rev. Mod. Phys. **69**, 629–642 (1997).

[4] M. Bulatowicz, R. Griffith, M. Larsen, J. Mirijanian, C. B. Fu, E. Smith, W. M. Snow, H. Yan, and T. G. Walker, "Laboratory search for a long-range t-odd, p-odd interaction from axionlike particles using dual-species nuclear magnetic resonance with polarized ^{129}Xe and ^{131}Xe gas," Phys. Rev. Lett. **111**, 102001 (2013).

[5] Junyi Lee, Attaallah Almasi, and Michael Romalis, "Improved limits on spin-mass interactions," Phys. Rev. Lett. **120**, 161801 (2018).

[6] F. Allmendinger, W. Heil, S. Karpuk, W. Kilian, A. Scharth, U. Schmidt, A. Schnabel, Yu. Sobolev, and K. Tullney, "New limit on lorentz-invariance- and *cpt*-violating neutron spin interactions using a free-spin-precession ^{3}He-^{129}Xe comagnetometer," Phys. Rev. Lett. **112**, 110801 (2014).

[7] Michael V. Romalis, Dong Sheng, Brian Saam, and Thad G. Walker, "Comment on "new limit on lorentz-invariance- and *cpt*-violating neutron spin interactions using a free-spin-precession ^{3}He–^{129}Xe comagnetometer"," Phys. Rev. Lett. **113**, 188901 (2014).

[8] M. Smiciklas, J. M. Brown, L. W. Cheuk, S. J. Smullin, and M. V. Romalis, "New test of local lorentz invariance using a ^{21}Ne-Rb-K comagnetometer," Phys. Rev. Lett. **107**, 171604 (2011).

[9] J. M. Brown, S. J. Smullin, T. W. Kornack, and M. V. Romalis, "New limit on lorentz- and *cpt*-violating neutron spin interactions," Phys. Rev. Lett. **105**, 151604 (2010).

[10] Alexander G. Glenday, Claire E. Cramer, David F. Phillips, and Ronald L. Walsworth, "Limits on anomalous spin-spin couplings between neutrons," Phys. Rev. Lett. **101**, 261801 (2008).

[11] M. A. Rosenberry and T. E. Chupp, "Atomic electric dipole moment measurement using spin exchange pumped masers of ^{129}Xe and ^{3}He," Phys. Rev. Lett. **86**, 22–25 (2001).

[12] F. Allmendinger, I. Engin, W. Heil, S. Karpuk, H.-J. Krause, B. Niederländer, A. Offenhäusser, M. Repetto, U. Schmidt, and S. Zimmer, "Measurement of the permanent electric dipole moment of the ^{129}Xe atom," Phys. Rev. A **100**, 022505 (2019).

[13] N. Sachdeva, I. Fan, E. Babcock, M. Burghoff, T. E. Chupp, S. Degenkolb, P. Fierlinger, S. Haude, E. Kraegeloh, W. Kilian, S. Knappe-GrÃijneberg, F. Kuchler, T. Liu, M. Marino, J. Meinel, K. Rolfs, Z. Salhi, A. Schnabel, J. T. Singh, S. Stuiber, W. A. Terrano, L. Trahms, and J. Voigt, "New limit on the permanent electric dipole moment of ^{129}xe using ^{3}he comagnetometry and squid detection," (2019), arXiv:1909.12800 [physics.atom-ph].

[14] T W Kornack, R. Ghosh, and M. V. Romalis, "Nuclear spin gyroscope based on an atomic comagnetometer," Physical review letters **95**, 230801 (2005).

[15] Liwei Jiang, Wei Quan, Rujie Li, Wenfeng Fan, Feng Liu, Jie Qin, Shuangai Wan, and Jiancheng Fang, "A parametrically modulated dual-axis atomic spin gyroscope," Applied Physics Letters **112**, 054103 (2018), https://doi.org/10.1063/1.5018015.

[16] F. A. Karwacki, "Nuclear magnetic resonance gyro development," Navigation **27**, 72 (1980).

[17] E.A. Donley, "Nuclear magnetic resonance gyroscopes," in *Sensors, 2010 IEEE* (2010) pp. 17 –22.

[18] M. E. Limes, N. Dural, M. V. Romalis, E. L. Foley, T. W. Kornack, A. Nelson, L. R. Grisham, and J. Vaara, "Dipolar and scalar ^{3}He–^{129}Xe frequency shifts in stemless cells," Phys. Rev. A **100**, 010501 (2019).

[19] W. A. Terrano, J. Meinel, N. Sachdeva, T. E. Chupp, S. Degenkolb, P. Fierlinger, F. Kuchler, and J. T. Singh, "Frequency shifts in noble-gas comagnetometers," Phys. Rev. A **100**, 012502 (2019).

[20] V. I. Petrov, A. S. Pazgalev, and A. K. Vershovskii, "Isotope shift of nuclear magnetic resonances in 129xe and 131xe caused by spin-exchange pumping by alkali metal atoms," (2019), arXiv:1906.06556 [physics.atom-ph].

[21] T. E. Chupp, E. R. Oteiza, J. M. Richardson, and T. R. White, "Precision frequency measurements with polarized ^{3}He, ^{21}Ne, and ^{129}Xe atoms," Phys. Rev. A **38**, 3998–4003 (1988).

[22] D. Brinkmann, E. Brun, and H. H. Staub, "Kernresonanz im gasformigen xenon," Helv. Phys. Acta **35**, 431 (1962).

[23] A. Korver, D. Thrasher, M. Bulatowicz, and T. G. Walker, "Synchronous spin-exchange optical pumping," Phys. Rev. Lett. **115**, 253001 (2015).

[24] T. M. Kwon, J. G. Mark, and C. H. Volk, "Quadrupole nuclear spin relaxation of ^{131}Xe in the presence of rubidium vapor," Phys. Rev. A **24**, 1894–1903 (1981).

[25] A. Korver, R. Wyllie, B. Lancor, and T. G. Walker, "Suppression of spin-exchange relaxation using pulsed parametric resonance," Phys. Rev. Lett. **111**, 043002 (2013).

[26] N. D. Bhaskar, M. Hou, M. Ligare, B. Suleman, and W. Happer, "Role of na-xe molecules in spin relaxation of optically pumped na in xe gas," Phys. Rev. A **22**, 2710–2716 (1980).

[27] E. Babcock, B. Chann, T. G. Walker, W. C. Chen, and T. R. Gentile, "Limits to the polarization for spin-exchange optical pumping of ^{3}He," Phys. Rev. Lett. **96**, 083003 (2006).

[28] Z. Wu, S. Schaefer, G. D. Cates, and W. Happer, "Coherent interactions of the polarized nuclear spins of gaseous atoms with the container walls," Phys. Rev. A **37**, 1161–1175 (1988).

[29] John Bechhoefer, "Feedback for physicists: A tutorial essay on control," Rev. Mod. Phys. **77**, 783–836 (2005).

[30] D.W. Allan and J.A. Barnes, "A modified "allan variance" with increased oscillator characterization ability," Proceedings of the 35th Anual Frequency Control Symposium , 470–475 (1981).

[31] J. Vanier and C. Audoin, "Electromagnetic and noise concepts," in *The Quantum Physics of Atomic Frequency Standards*, Vol. 2 (IOP Publishing Ltd, 1989) Chap. Appendix 2F, pp. 216–256.

[32] Juha Vaara and Michael V. Romalis, "Calculation of scalar nuclear spin-spin coupling in a noble-gas mixture," Phys. Rev. A **99**, 060501 (2019).